Desalination and Water Treatment
www.deswater.com
doi: 10.1080/19443994.2014.934725

56 (2015) 239–247
September

Taylor & Francis
Taylor & Francis Group

Novel Co/Mo layered double hydroxide: synthesis and uptake of Fe(II) from aqueous solutions (Part 1)

M.S. Mostafa[a], A.A. Bakr[b,*], Gh. Eshaq[c], M.M. Kamel[d]

[a]*Department of Refining, Egyptian Petroleum Research Institute (EPRI), Nasr City, Cairo 11727, Egypt, Tel. +00201114502512; email: mohsendib@yahoo.com*
[b]*Department of Analysis and Evaluation, Egyptian Petroleum Research Institute (EPRI), Nasr City, Cairo 11727, Egypt, Tel. +00201227135228; email: als_water@yahoo.com*
[c]*Department of Petrochemicals, Egyptian Petroleum Research Institute (EPRI), Nasr City, Cairo 11727, Egypt, Tel. +00201003056808; email: ghadaamer2002@yahoo.com*
[d]*Faculty of Science, Department of Chemistry, Al-Azhar University, Assuit Branch, Assuit City, Egypt, Tel. +00201113033830; email: mmk.electro@yahoo.com*

Received 17 November 2013; Accepted 1 June 2014

ABSTRACT

A new type of M^{2+}/M^{6+}-LDH was prepared by the intercalation of Co/Mo-LDH with carbonate $(CO_3)^{2-}$ as an interlayer anion through a precise control of the titration rate of the alkaline solution into the cobalt and molybdenum cations. From the analytical results, the structure, composition and morphology of the prepared material were approved by XPS, XRD, FT-IR, N_2 adsorption–desorption isotherm, SEM, and DSC-TGA. The synthesized Co/Mo-LDH was applied to the removal of ferrous ions from aqueous solutions at ambient temperature, different pH, constant stirring at 160 rpm and different iron/adsorbent ratios. According to the experimental data, we have succeeded to prepare a novel adsorbent for Fe(II) uptake and at pH 5, stirring at 160 rpm, and after 60 min the uptake reached a maximum value of 10 mg/g of Co/Mo-LDH. Hence, the higher adsorption capacity of the Co/Mo-LDH was explained by the formation of 4^+ surface charges between Co^{2+} and Mo^{6+} which produced a highly energetic surface layers as detected by XPS.

Keywords: Layered double hydroxide; Nano-materials; Fe(II) adsorption; Water treatment

1. Introduction

It is well known that the most dominant form of dissolved iron is the soluble Fe^{+2} ions at a pH range from 5 to 8. Therefore, when the iron is present as soluble form in drinking water supplies, there are many objectionable problems related to its presence taking place [1]. The European Union has recommended the level of 0.2 mg/l for iron [2], while the environmental protection agency (EPA) has established the secondary standards of 0.3 mg/l for iron [3]. Hence, the presence of iron has been giving rise to serious problems for regulatory authorities related to the industrial and main water supplies for a long time [4]. The higher dissolved concentrations of iron have not any serious harm to human or animal health, but they cause aesthetic problems [5]. Bakr et al. have found that the removal of iron in the ground and seawater desalination plants is the key step in the designing of the

*Corresponding author.

plants to avoid RO membrane fouling and scaling which are the most serious problems in membrane processes [6,7]. Various treatment methods such as chemical precipitation, reverse osmosis, ion exchange, solvent extraction, coagulation, and adsorption were utilized to remove metal ions from aqueous solutions. However, due to the economic constraints of all these methods, the adsorption process is the most effective one, especially for effluents with moderate and low concentrations [8]. Since, the efficiency of adsorption depends on many factors, including the surface area, pore size distribution, polarity, and functional groups of the adsorbent [9], the nano-adsorbents are quite efficient for the fast adsorption of heavy-metal ions and organic molecules from aqueous solutions related to their high specific surface areas and absence of internal diffusion resistances [10].

Recently, the layered double hydroxides (LDHs), also known as hydrotalcites (HTs) or anionic clays, have also deserved interest due to their large ionic exchange capacities [11]. LDH has a general formula of $[M^{2+}_{(1-X)}\ M^{3+}_{X}\ (OH)_2]^{X+}\ (A^-)^x n{\cdot}H_2O$ where M^{2+} and M^{3+} represent the divalent and trivalent metal cations, x is the mole percent of M^{3+} i.e. $M^{3+}/M^{2+}+M^{3+}$ ranges typically from 0.18 to 0.33 producing a variety of iso-structural materials, A is the interlayer anion and n represents the number of water molecules. The creation of such positive charge is the key factor in LDH to intercalate and exchange different organic and inorganic anions [12]. The use of HTs for the water purification is well understood and mainly progressed to improve their efficiency, specificity, and applications. The LDH is a class of lamellar ionic compounds containing a positively charged layer and exchangeable anions in the interlayer and some LDHs containing varying amounts of Al^{3+}, Zr^{4+}, and Zn^{2+} or Mg^{2+} in the metal hydroxide layer for Cr(VI) and Se(IV) adsorption [13]. There are different types of LDHs samples that have been synthesized with carbonate as an interlayer anion such as MgAl, ZnAl, and MgAlFe. LDHs samples following a standard co-precipitation method from the metal chlorides have been evaluated in the adsorptive removal of Cr(VI) from aqueous solutions [11]. Also, the removal percentage of the initial Fe^{+2} concentration 200 ppm from aqueous solution was 85% by using the synthesized zaccagnaite (as LDH) and it was one of the best adsorbents for the removal of Cu^{2+}, Fe^{2+} and Mn^{2+} [1].

While, the ordinary LDH is usually prepared from divalent and trivalent cations, the first aim of this study was to prepare the Co/Mo(CO_3^{2-})-LDH from bivalent and hexavalent cations as a new type of LDH by precise controlling the addition rates of the alkaline solution (ammonium hydroxide and ammonium carbonate) against the Co and Mo cations. While the second aim was to apply this novel LDH nanoparticles to the Fe(II) removal from aqueous solutions and determine the adsorption rate and the capacity of Co/Mo-LDH. Thereafter, we are looking forward to study, in other late studies, the kinetics and thermodynamics of Fe(II) removal by un-calcined and calcined Co/Mo-LDHs.

2. Materials and methods

2.1. Materials

All chemicals with a purity greater than 99.9% were purchased as follows: Ferrous Sulfate ($FeSO_4{\cdot}7H_2O$) was purchased from Loba Chemie Co., anhydrous ($MoCl_5$), $CoCl_2{\cdot}6H_2O$, and ammonium carbonate $(NH_4)_2CO_3$ were purchased from Sigma-Aldrich (Germany) and NH_4OH (34%) was purchased from Merck Germany.

2.2. Preparation of Co/Mo-LDH

Adjustable co-precipitation method was performed for the preparation of Co/Mo(CO_3)$^{2-}$-LDH by increasing the addition rate of NH_4OH and $(NH_4)_2CO_3$ into the Co and Mo cations at 60°C. Firstly, a solution A ($MoCl_5$ and $CoCl_2{\cdot}6H_2O$) with total concentration 59 mmol and molar coefficient 0.25 was prepared in 100 ml de-ionized water, while a second solution B was prepared from NH_4OH (10 mmol) and $(NH_4)_2CO_3$ (20 mmol) in 50 ml de-ionized water. The amount of solution B required to reach a pH 8–9 was well known and the addition rate of this amount successively to solution A was adjusted to the aging time of 24 h at temperature 60°C under vigorous stirring.

2.3. Characterization of Co/Mo-LDH

The oxidation state of Mo in the synthesized Co/Mo-LDH was determined using thermo scientific X-ray photoelectron spectroscopy XPS model K-Alpha (England). X-ray powder diffraction (XRD) patterns were recorded on a Brucker AXS-D8 Advance (Germany) by using nickel-filtered copper radiation ($\lambda = 1.5405$ Å) at 60 kV and 25 mA with scanning speed of 8° in 20 min^{-1} over diffraction angle range. While the elemental analysis of Co/Mo-LDH before and after adsorption procedures of Fe(II) was performed by X-ray fluorescence (XRF) instrument with channel control model Pw1390 (Philips) and spectrometer model Pw 1410, involving determination of Co, Mo and/or Fe (II) contents. Surface area and pore volume was determined from nitrogen adsorption–desorption isotherms

of the linear BET plots using Quantachrome Nova 3200 Instrument (USA). Before the measuring procedure, the sample was degassed at 60 ℃ for 2 h under vacuum to remove the contaminated non-interlayer water while conserving the parental Co/Mo-LDH structure. The degassing degree was chosen according to the DSC-TGA results. Fourier transfer infrared (FT-IR) spectra were recorded on ATI Mattson Genesis series (KBr disc method) apparatus, Model 960 M009 series. Thereafter, differential scanning calorimeter (DSC) was used to determine the change in the structure accompanying the thermal treatment using SDT-Q600 V20.5 Pouild 15 apparatus, thermo-gravimetric analysis (TGA) was also performed. Finally, the morphological features of the prepared sample were analyzed by scanning electron microscope (SEM) using JEOL 5300 SEM instrument (Japan).

2.4. Adsorption experiments

According to the experimental studies, the high ferrous ions stock solution of concentration 100 mg/l was prepared by dissolving Ferrous Sulfate in distilled water. The Fe(II) solution concentration ranging from 1 to 25 mg/l for all experiments was prepared from the stock solution. The standard acid (0.01 M HNO_3) and alkaline solutions (0.125 M NaOH) were used for pH adjustments at different pH values 3, 4, 5, 6, 7, 8, 9, and 10. Thereafter, the pH value of the solution was measured using a pH meter (Mettler-Toledo AG 8603 Schwerzenbach, made by Mettler-Toledo Group) and the pH meter was calibrated with buffers of pH 4 and 7 before any measurement.

The removal of ferrous ions from dilute aqueous solutions by adding adsorbent (Co/Mo-LDH) doses 0.01, 0.02, 0.03, 0.04, and 0.05 g/l were carried out at a constant temperature 25 ℃. A constant continuous stirring was done over a magnetic stirrer at 160 rpm for a predetermined time interval (5, 10, 15, 20, 30, 45, and 60 min) to allow the dispersion of adsorbent and metal ions reach the equilibrium. The solid and solution were separated by centrifugation at 3,000 rpm for 15 min and the solid was slightly dried at ambient temperature. The Fe(II) ions concentrations were determined by Spectrophotometer, LaMotte, model SMART Spectro, USA and the solid phase was then analyzed. Thereafter, the amount of adsorption q_e (mg/g) and the removal percentage (% removal) were calculated by the following equations [14]:

$$q_e = (C_0 - C_e) \times V/m \quad (1)$$

$$\%\,\text{removal} = (C_0 - C_e)/C_0 \times 100\% \quad (2)$$

where C_0 and C_e are the initial Fe(II) concentration and the concentration at equilibrium in mg/l, m is the mass of adsorbent and V is the volume of solution.

2.5. Effect of initial solution pH

The effect of initial solution pH on ferrous adsorption was evaluated using a series of 2 mg/l Fe(II) solutions at a constant adsorbent dosage 0.02 g/l and the starting solution pH was adjusted to the designed values (3, 4, 5, 6, 7, 8, 9, and 10). Thereafter, the resulting Co/Mo-LDHs suspensions were filtered and then the residual Fe(II) concentrations were analyzed.

2.6. Effect of adsorbent dosage

Different amounts of Co/Mo-LDHs (0.01, 0.02, 0.03, 0.04, and 0.05 g/l) were added to a series of 100 ml of ferrous solutions at constant initial concentration 2 mg/l, pH 5, and stirring at 160 rpm for different contact times (5, 10, 15, 20, 30, 45, and 60 min) to reach the equilibrium. Then the aqueous samples were filtered and the residual Fe(II) concentrations were analyzed.

3. Results and discussion

3.1. Characterization of Co/Mo-LDH

3.1.1. XPS analysis

X-ray photoelectron spectroscopy XPS illustrated the presence of Mo in its oxidation state Mo^{6+} (i.e. oxidation of Mo^{5+} during the preparation process) where the electron binding energy of Mo (3*d*) for the synthesized Co/Mo-LDH was 231.90 eV and it was very close to 231.6–232.7 eV of Mo^{6+} (MoO_3) as shown in Fig. 1. Therefore, the XPS data confirmed the synthesis of the new Co/Mo-LDH which consists of bivalent and hexavalent cations.

3.1.2. Elemental analysis

The XRF showed that, the percentage of Co to Mo in the mother freshly synthesized Co/Mo-LDH was 2.92:1 and it was closed to 3:1 in the initial solution. This variation was found previously [15,16] and may be due to lack of precipitation. Taking into account the general formula of the LDHs is $[M^{2+}_{(1-X)}\ M^{3+}_{X}\ (OH)_2]^{X+}\ (A^-)^x n{\cdot}H_2O$, the chemical composition of the synthesized Co/Mo-LDH can be stated as $[Co_{0.75}\ Mo_{0.25}\ (OH)_2]^{0.25}\ (CO_3^{2-})_{0.125}\ n{\cdot}H_2O$.

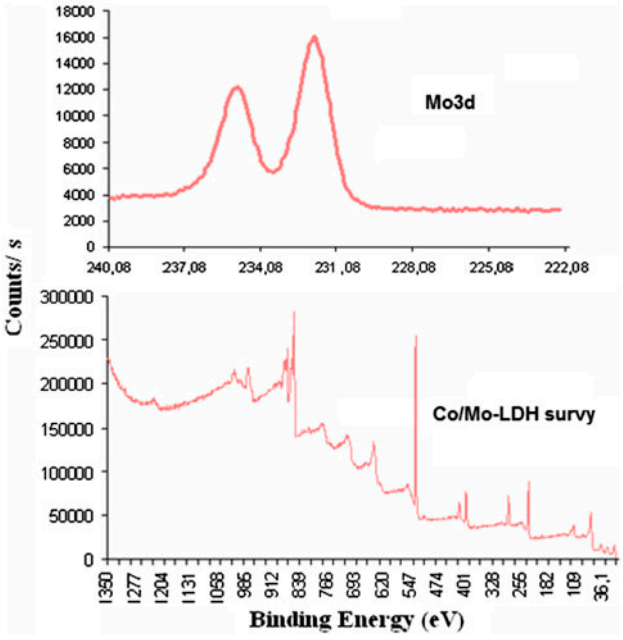

Fig. 1. XPS spectra of synthesized Co/Mo-LDH.

3.1.3. XRD analysis

The X-ray powder diffraction pattern of Co/Mo-LDH is shown in Fig. 2. The pattern shows that the HT structure of Co/Mo-LDH as the only crystalline component (JCPDS file no. 22-700) exhibited a sharp and symmetric reflection of the basal (0 0 3), (0 0 6) and (0 0 9) planes, and asymmetric reflections for non-basal (0 1 2), (0 1 5) and (0 1 8) planes. The good agreement between the values corresponding to successive diffractions by basal planes, i.e. $d(0\,0\,3) = 2d(0\,0\,6) = 3d(0\,0\,9)$ for Co/Mo-LDH, reveals highly packed stacks of brucite-like layers ordered along axis *c*. The parameter "*c*" is related to the thickness of the brucite-like layer and the interlayer distance, is commonly calculated as three times the spacing for plane (0 0 3), i.e. 2.27 nm. The *c* dimension was much closer to that reported for natural and synthetic HT, 2.31 nm [17–19]. The Co/Mo-LDH X-ray diffraction patterns has the main peak at 0.68 nm which is a small peak compared to 0.76 nm for any M^{2+}/M^{3+} LDH which can be explained by the formation of 4^+ charges in Co/Mo-LDH instead of 2^+ in case of the conventional LDHs. Also, the possibility of the electrostatic interaction between the inorganic layer and guest compounds was stronger than that for the commons.

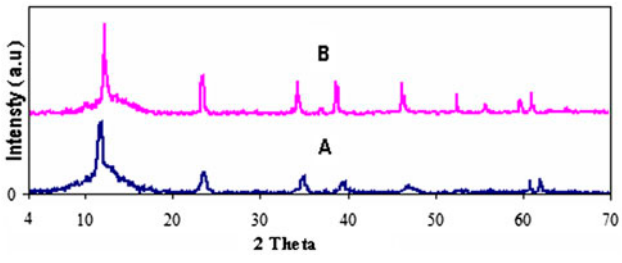

Fig. 2. XRD patterns of Co/Mo-LDH (A) before and (B) after adsorption.

3.1.4. FTIR spectroscopy

FTIR spectra of the synthesized Co/Mo$(CO_3)^{2-}$-LDH are shown in Fig. 3. The obtained spectra were the characteristics of the well-known HT like compounds with $(CO_3)^{2-}$ as an interlayer anion [15,20]. The presence of carbonate group in the interlayer can be observed by the absorption band near 1,380 cm^{-1} related to the asymmetric stretching ($\upsilon 3$) of the $(CO_3)^{2-}$ species associated with its companion approximately at 1,510 cm^{-1}. This band was recorded at 1,450 cm^{-1} for free carbonate species, while it splits and shifts upon symmetry lowering, the splitting here was perhaps due to the restricted symmetry in the interlayer space and the different electrostatic interactions. An extremely broad band between 3,600 and 3,200 cm^{-1} is due to the OH stretching mode of hydroxyl group layers and interlayer water molecules. This broadness of the OH band may be due to the presence of hydrogen bonding [16,21,22], while the weak shoulder peak occurs approximately at 3,000 cm^{-1} is attributed to the OH stretching mode of interlayer water molecules hydrogen-bonded to interlayer anions. The weak band around 1,600 cm^{-1} is related to the bending mode band of water molecules [23]. Characteristics peaks for O–Mo–O, Mo–O–Co and Co–OH can be represented by the weak bands in the low frequency region (1,000–500 cm^{-1}) [19,24].

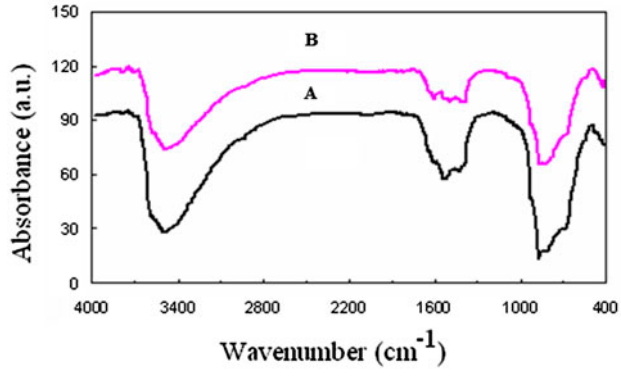

Fig. 3. FT-IR spectra of Co/Mo-LDHs (A) before and (B) after adsorption.

3.1.5. Surface area and pore size distribution

The N_2 adsorption–desorption isotherm of the prepared Co/Mo-LDH is shown in Fig. 4. It is clear that it exhibits a type IV isotherm according to the IUPAC classification with a hystersis loop for the desorption isotherm closed at a relative pressure P/Po in range 0.4–0.95, this type of isotherm is related to mesoporous materials [25]. The N_2 uptake took place at P/Po higher than 0.02, which means that the interstitial micropores are blocked, consequently, the interlamellar space of the freshly prepared Co/Mo-LDH under investigation (degassing at 60°C for 2 h to ensure a parental structure of LDH) is completely occupied by the interlayer water molecules and the carbonate anion. By the multi-point BET and BJH methods the surface area and pore size distribution were determined, where the BJH methods and t-plot method were used to calculate the micropore volume. As shown in Table 1, the synthesized Co/Mo-LDH under investigation has a surface area of 64.7 m^2/g, pore volume of 0.163 ml/g, average pore size of 10.54 nm and completely absence of microporosity. The value of 64.7 m^2/g surface area for Co/Mo-LDH under such condition of degassing prior to N_2 adsorption–desorption isotherm can be considered as a good and promising value beside the full mesoporosity of the sample.

3.1.6. Thermal analysis

The DSC–TGA thermograph of Co/Mo-LDH is shown in Fig. 5. Firstly, no exothermic peaks related to the oxidation of Mo^{+5} (starting material) to Mo^{+6} (LDH product) indicated the completion of this step during the experimental procedure and this in accordance with the XPS data, beside, the shown DSC-TGA is similar to that characteristic for ordinary LDHs [26]. Secondly, the Co/Mo-LDH showed two LDH characteristic weight losses one at 145°C accompanied with an endothermic peak at 87°C related to the surface adsorbed water removal and another at 364°C accompanied with an endothermic peak at 318°C corresponding to the removal of the interlayer water, carbonate anion, and complete dehydroxylation of the brucite layers.

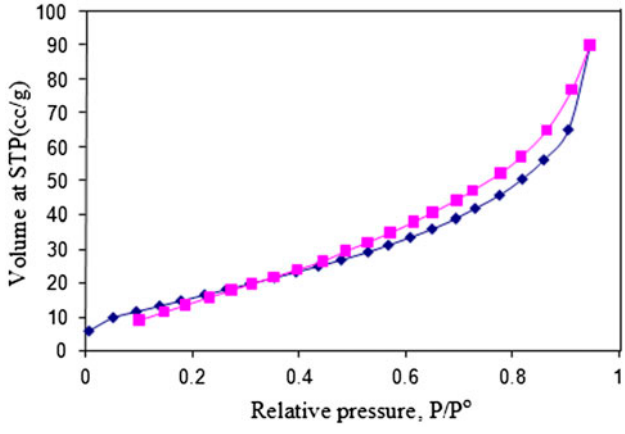

Fig. 4. N_2 adsorption–desorption isotherm.

3.1.7. SEM images

The Co/Mo-LDH SEM images before and after Fe (II) adsorption are shown in Fig. 6(a) and (b). The prepared sample exhibited a plate-like morphology and hexagonal crystallite which is the general characteristic of the LDH crystallite.

3.2. Effect of initial Fe(II) concentration

The effect of different Fe(II) concentrations was determined after experimental studies for a range of metal concentrations. A definite dosage of Co/Mo-LDH adsorbent 0.02 g/l was added to a series of 100 ml of ferrous solutions with the different initial concentrations of 1, 2, 3, 5, 8, 10, 15, 20, and 25 mg/l at constant pH 5, stirring at 160 rpm and contact time 60 min to reach the equilibrium. The Fe(II) removal is shown in Fig. 7 which indicated that the Co/Mo-LDH apparently removed a considerable amount of ferrous from the aqueous solutions. The adsorption efficiency increased to a certain level and the saturation occurred when no more metal ions could be adsorbed on the surface of Co/Mo-LDH. The experimental studies also showed a high efficiency for ferrous adsorption and it was obtained through a relatively short period of time up to 60 min. However, the complete removal of ferrous was observed at initial concentrations of 1.0, 2.0, 3.0, and also 5.0 mg/l.

3.3. Effect of contact time

Fig. 8 shows the effect of contact time on the adsorption capacity and the percentage removal of initial Fe(II) concentration 2.0 mg/l using 0.02 g/l Co/Mo-LDH at pH 5, stirring at 160 rpm and temperature 25°C. It was noted that the adsorption rate was considerably fast within the first 20 min (7.55 mg of Fe (II) adsorbed per gram of Co/Mo-LDH), then gradually slowed down and thereafter, the adsorption equilibrium was reached within 60 min (10.0 mg). The fast rate of Fe(II) removal in the beginning may be attributed to the rapid diffusion of Fe(II) from the solution

Table 1
N_2 adsorption–desorption data

Sample	BET area (m^2/g)	C-value in BET equation	Pores volume (ml/g)	Average pore size (nm)	Micropore volume (ml/g)
Co/Mo-LDH	64.7	23	0.163	10.54	0.0

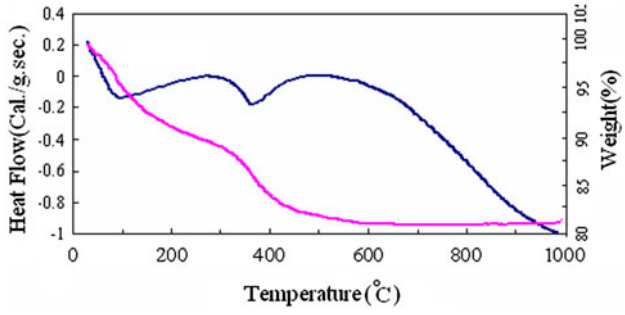

to the external surfaces of Co/Mo-LDH. On the other hand, the slow adsorption process attributed to the longer diffusion range of Fe(II) into the inner-sphere of Co/Mo-LDH or to the ion-exchange in the inner surface of Co/Mo-LDH. Such slow diffusion will lead to a slow increase in the adsorption curve at later stages [27]. Moreover, the initial rapid adsorption may be related to the increase in the available sites at the initial stage. Hence, the higher adsorption capacity of the Co/Mo-LDH was explained by the formation of 4^+ surface charges between the bivalent and hexavalent

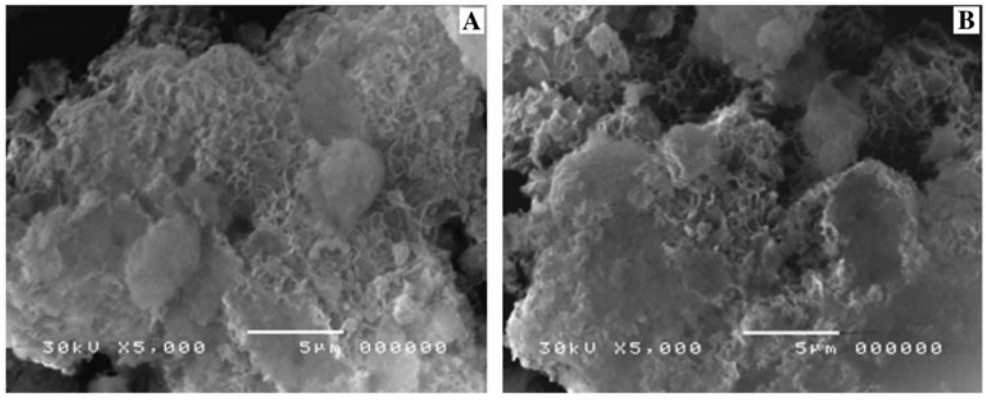

Fig. 6. SEM images: (A) before and (B) after adsorption.

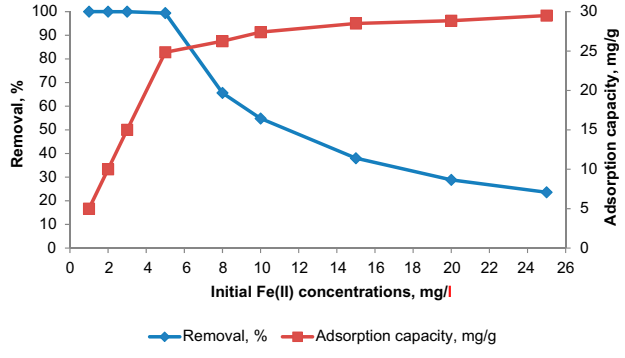

Fig. 7. Effect of Fe(II) initial concentration on the percentage of Fe(II) removal and adsorption capacity (mg/g).

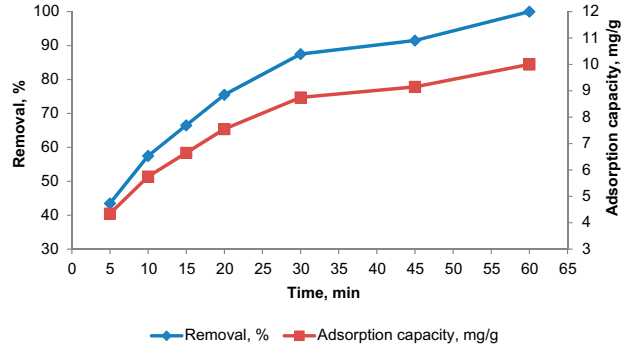

Fig. 8. Effect of contact time on the percentage of Fe(II) removal and adsorption capacity (mg/g).

cations (Co^{2+} and Mo^{6+}) which produced highly energetic surface layers as detected by XPS, Fig. 1.

3.4. Effect of initial solution pH

The effect of the starting solution pH on the Fe(II) removal from aqueous solutions with an initial concentration 2.0 mg/l onto 0.01, 0.02, 0.03, 0.04, and 0.05 g/l Co/Mo-LDH for 60 min is shown in Fig. 9. The obtained data indicated that the amounts of Fe(II) adsorbed on Co/Mo-LDH decreased with decreasing the starting solution pH (pH ≤ 4), while at pH > 4, the removal of Fe(II) seemed to be pH-independent. Since, the decrease in the Fe(II) removal at low-pH range may be due to the dissolution of LDH in the low-pH solutions [28]. It was confirmed by the presence of Co and Mo in the final solution by the spectrophotometeric analysis.

From Fig. 9, the adsorption of a constant Fe(II) concentration 2.0 mg/l on different LDH doses showed the same behavior with respect to the starting solution pH. For Co/Mo-LDH dosages 0.01, 0.02, 0.03, 0.04, and 0.05 g/l, the removal percentages of 2.0 mg/l Fe(II) were 48–92 in a starting pH values from 3 to 4. At higher pH (pH ≥ 4), the Fe(II) adsorption increased with increasing pH and reached its maximum value at pH 5 (100%) even at low dosage 0.02 g/l. Thereafter, the removal decreased and appeared to reach a plateau region at the pH range 6–8 at lower dosage 0.01 g/l from 74 to 84%. Then, the adsorption decreased again with increasing pH (above 8) to reach 44–52% at dosage 0.01 g/l. Finally, the lower adsorption at the higher pH range may be due to the increase of competitive effect of OH-adsorption on LDH [29].

3.5. Effect of LDH dosage

Different amounts of Co/Mo-LDHs (0.01, 0.02, 0.03, 0.04, and 0.05 g/l) were added to a series of 100 ml of ferrous solutions with initial concentration of 2 mg/l at pH 5, stirring at 160 rpm and contact time 60 min to reach the equilibrium. Then, the aqueous samples were filtered and the residual Fe(II) concentrations were analyzed.

The effect of the LDH adsorbent dosages (0.01, 0.02, 0.03, 0.04, and 0.05 g/l) on the Fe(II) adsorption concentration 2 mg/l is shown in Fig. 10. From these experiments, the metal solutions containing the appropriate adsorbent dose were loaded in 100 ml snap-seal polyethylene bottles, which were then stirred at 160 rpm for 60 min. Then, the mixture in each bottle was centrifuged immediately and the Fe(II) concentrations in the supernatant solutions were determined by Spectrophotometer. As expected, the percentage of Fe(II) removal firstly increased sharply with increasing the LDH dose and then levels off at an adsorbent dose above 0.04 g/l. On the other hand, the loading capacity of the material decreases with increasing the LDH dose, as represented by Das et al. [30].

Even at the lower LDH dosage 0.01 g/l, the ferrous concentration value after adsorption was lower than 0.3 mg/l and it can meet the standard of the iron limit for drinking water by the EPA [3]. While, when the adsorbent dosage was ≥0.02 g/l, the ferrous concentration after adsorption was lower than 0.2 mg/l and it can meet the standard of the iron limit for drinking water by the European Union [2].

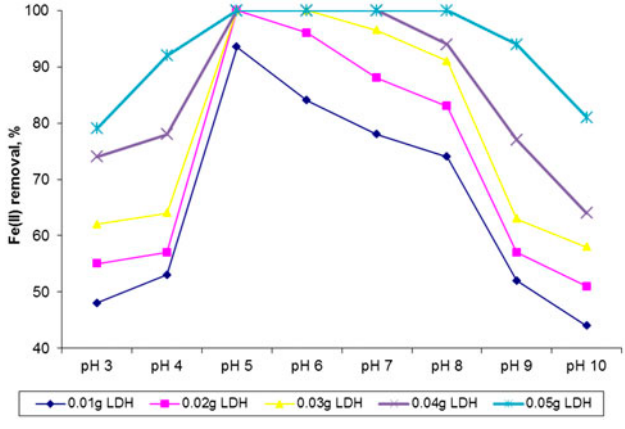

Fig. 9. Effect of initial solution pH on removal percentage of 2.0 mg/l Fe(II) concentration at different adsorbent dosages.

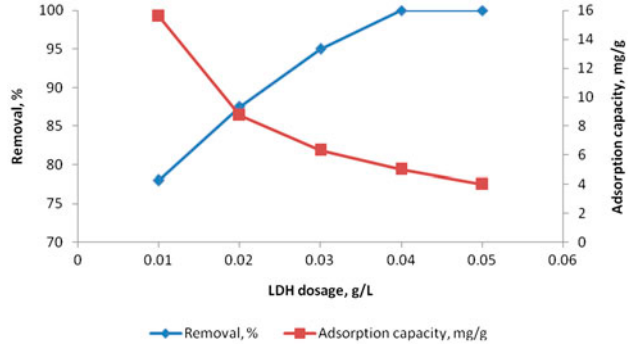

Fig. 10. Co/Mo-LDH adsorbent dosages as a function of Fe(II) adsorption: initial ferrous concentration 2.0 mg/l, pH 5.0 and temperature 25˚C.

4. Conclusions

A novel Co/Mo-LDH intercalated with carbonate $(CO_3)^{2-}$ as an interlayer anion was successfully synthesized by co-precipitation method and its structure was well characterized by XPS, XRD, FT-IR, N_2 adsorption–desorption isotherm, SEM, and DSC-TGA. The present study showed that Co/Mo-LDH was a suitable adsorbent for the Fe(II) removal from aqueous solutions. The removal of ferrous ions was found to be dependent on pH, contact time, adsorbent dosage and initial adsorbate concentration. The above obtained results consistently suggested that the higher adsorption capacity of the Co/Mo-LDH was explained by the formation of 4^+ surface charges between Co^{2+} and Mo^{6+} which produced a highly energetic surface layers as detected by XPS.

Acknowledgments

The authors express their thanks and appreciation to Prof. Dr Naglaa Ali, Egyptian Petroleum Research Institute (EPRI) and Ahmed Ezzat ElMetwally, Petrochemical Technology Lab., EPRI, for their assistance and revision of this paper.

References

[1] A. Jaiswal, M.C. Chattopadhyaya, Interaction of Mn^{2+}, Fe^{2+} and Cu^{2+} heavy metal ions from aqueous solution by zaccagnaite, a hydrotalcite-like compound, Desalin. Water Treat. 29 (2011) 252–257.
[2] European Union, Richtlinie, 98/83/EG des Rates, 1998.
[3] U.S. EPA, Office of Water, National Secondary Drinking Water Regulations, Code of Federal Regulation, 2001, pp. 612–614. Available from: https://info.ngwa.org/GWOL/pdf/012972267.pdf?origin=publication_detail.
[4] P. Jaudon, Groundwater pollution by manganese. Manganese speciation: Application to the selection and discussion of an *in situ* groundwater treatment, Sci. Total Environ. 84 (1989) 169–183.
[5] P. Maloszewski, S. Witczak, G. Malina, Groundwater Quality Sustainability, CRC Press/Balkema, Boca Raton, FL, 2012.
[6] A.A. Bakr, M.M. Kamel, A. Hamdy, Z.M. Khaled, M.A. Abbas, Reverse osmosis pretreatment: Removal of iron in groundwater desalination plant in Shupramant-Giza—A case study, Curr. World Environ. 7 (2012) 23–32.
[7] A.A. Bakr, W.A. Makled, New pretreatment media-filtration for SWRO membranes of desalination plants, in: 13th International Conference on Environmental Science and Technology, CEST2013_0065, 5–7 September, Athens, Greece, 2013.
[8] D.M. Manohar, B.F. Noeline, T.S. Anirudhan, Adsorption performance of Al-pillared bentonite clay for the removal of cobalt(II) from aqueous phase, Appl. Catal. Sci. 31 (2006) 194–206.
[9] A. Ewecharoen, P. Thiravetyan, E. Wendel, H. Bertagnolli, Nickel adsorption by sodium polyacrylate-grafted activated carbon, J. Hazard. Mater. 171 (2009) 335–339.
[10] S. Zhang, F. Cheng, Z. Tao, F. Gao, J. Chen, Removal of nickel ions from wastewater by $Mg(OH)_2$/MgO nanostructures embedded in Al_2O_3 membranes, J. Alloys Compd. 426 (2006) 281–285.
[11] D. Carriazo, M.D. Arco, C. Martín, V. Rives, A comparative study between chloride and calcined carbonate hydrotalcites as adsorbents for Cr(VI), Appl. Catal. Sci. 37 (2007) 231–239.
[12] S.J. Palmer, R.L. Frost, Use of hydrotalcites for the removal of toxic anions from aqueous solutions, Ind. Eng. Chem. Res. 49 (2010) 8969–8976.
[13] N.N. Das, J. Konar, M.K. Mohanta, S.C. Srivastava, Adsorption of Cr(VI) and Se(IV) from their aqueous solutions onto Zr^{4+}-substituted ZnAl/MgAl-layered double hydroxides: Effect of Zr^{4+} substitution in the layer, J. Colloid Interface Sci. 270 (2004) 1–8.
[14] A. Legrouri, M. Lakraimi, A. Barroug, A.D. De Roy, J.P. Besse, Removal of the herbicide 2,4-dichlorophenoxyacetate from water to zinc–aluminium–-chloride layered double hydroxides, Water Res. 39 (2005) 3441–3448.
[15] J.T. Kloprogge, R.L. Frost, Fourier transform infrared and raman spectroscopic study of the local structure of Mg-, Ni-, and Co-hydrotalcites, J. Solid State Chem. 146 (1999) 506–515.
[16] F. Cavani, F. Trifirò, A. Vaccari, Hydrotalcite-type anionic clays: Preparation, properties and applications, Catal. Today 11 (1991) 173–301.
[17] M. Intissar, R. Segni, C. Payen, J. Besse, F. Leroux, Trivalent cation substitution effect into layered double hydroxides $Co_2Fe_yAl_{1-y}(OH)_6Cl{\bullet}nH_2O$: Study of the local order, ionic conductivity and magnetic properties, J. Solid State Chem. 167 (2002) 508–516.
[18] F. Leroux, E.M. Moujahid, C. Taviot-Guého, Effect of layer charge modification for Co–Al layered double hydroxides: Study by X-ray absorption spectroscopy, Solid State Sci. 3 (2001) 81–92.
[19] N. Nakamoto, Infrared and Raman Spectra of Inorganic and Co-ordination Compounds, fourth ed., John Wiley & Sons, New York, NY, 1986.
[20] M.J. Hernandez-Moreno, M.A. Ulibarri, J.L. Rendon, C.J. Serna, IR characteristics of hydrotalcite-like compounds, Phys. Chem. Miner. 12 (1985) 34–38.
[21] A. Vaccari, Clays and catalysis: A promising future, Appl. Clay Sci. 14 (1999) 161–198.
[22] F.M. Labajos, V. Rives, M.A. Ulibarri, Effect of hydrothermal and thermal treatments on the physicochemical properties of Mg–Al hydrotalcite-like materials, J. Mat. Sci. 27 (1992) 1546–1552.
[23] J. Pérez-Ramírez, G. Mul, F. Kapteijn, J.A. Moulijn, In situ investigation of the thermal decomposition of Co–Al hydrotalcite in different atmospheres, J. Mater. Chem. 11 (2001) 821–830.
[24] A.M. El-Toni, S. Yin, T. Sato, Silica coating of Zn_2Al/4-hydroxy-3-methoxybenzoic acid nanocomposites via seeded polymerization technique, Mater. Chem. Phys. 89 (2005) 154–158.
[25] G.D. Wu, X. Wang, B. Chen, J.P. Li, N. Zhao, W. Wei, Y. Sun, Fluorine-modified mesoporous Mg–Al mixed oxides: Mild and stable base catalysts for O-methylation of

phenol with dimethyl carbonate, Appl. Catal., A 329 (2007) 106–111.
[26] S. Miyata, The synthesis of hydrotalcite-like compounds and their structures and physico-chemical properties. I: The systems Mg^{2+}–Al^{3+}–NO_3^-, Mg^{2+}–Al^{3+}–Cl^-, Mg^{2+}–Al^{3+}–ClO_4^-, Ni^{2+}–Al^{3+}–Cl^- and Zn^{2+}–Al^{3+}–Cl^-, Clays Clay Miner. 23 (1975) 369–375.
[27] M.H. Al-Qunaibit, W.K. Mekhemer, A.A. Zaghloul, The adsorption of Cu(II) ions on bentonite—A kinetic study, J. Colloid Interface Sci. 283 (2005) 316–321.
[28] M.C. Hermosín, I. Pavlovic, M.A. Ulibarri, J. Cornejo, Hydrotalcite as sorbent for trinitrophenol: Sorption capacity and mechanism, Water Res. 30 (1996) 171–177.
[29] L. Yang, Z. Shahrivari, P. Liu, M. Sahimi, T. Tsotsis, Removal of trace levels of arsenic and selenium from aqueous solutions by calcined and uncalcined layered double hydroxides (LDH), Ind. Eng. Chem. Res. 44 (2005) 6804–6815.
[30] D.P. Das, J. Das, K. Parida, Physicochemical characterization and adsorption behavior of calcined Zn/Al hydrotalcite-like compound (HTlc) towards removal of fluoride from aqueous solution, J. Colloid Interface Sci. 261 (2003) 213–220.